This article has been accepted for publication in a future issue of this journal, but has not been fully edited. Content may change prior to final publication. Citation information: DOI 10.1109/TWC.2022.3173207, IEEE Transactions on Wireless Communications



# On the Capacity of Index Modulation

Bharath Shamasundar, *Member, IEEE* and Aria Nosratinia, *Fellow, IEEE*

***Abstract*— Index modulation represents the transmitted information in two parts: by selecting a subset of available transmission dimensions (antennas, sub-carriers, or time-slots) whose selection index carries information, and by modulation symbols transmitted in the selected dimensions. Index modulation is motivated by reducing the transmitter hardware complexity and has attracted significant research attention in the past decade. In practice, knowing the spectral efficiency or capacity is essential for setting the parameters of modulation and coding for index modulation, but approximations and bounds thus far have not been accurate enough for that purpose. We calculate close lower and upper bounds for the spectral efficiency of index modulation. Our lower and upper bounds meet at high-SNR when the number of receive antennas is greater than or equal to the number of transmit antennas, thus the high-SNR capacity of index modulation in these cases has been fully characterized. A catalog of results is provided for spatial modulation, generalized spatial modulation, time and frequency index modulation. Extensive simulations illustrate the usefulness and accuracy of our results. For example, for spatial modulation with $4 \times 2$ antennas at 8 bits/s/Hz, our results are 2dB tighter than the best available bounds in the literature.**

## I. Introduction

Index modulation selects a subset of available transmission dimensions (antennas, sub-carriers, or time slots); the selection index carries part of the information to be communicated to the receiver. The remainder of information is conveyed by modulation symbols emitted in the selected dimensions [1], [2]. Spatial modulation is the most popular index modulation technique in which one out of $n_t$ available antennas is activated per channel use, and a modulation symbol is transmitted from the active antenna [3], [4]. Both the index of the active antenna and the transmitted symbol carry information. Spatial modulation is driven by the idea of utilizing the available multi-antenna channel while limiting complexity. Spatial modulation has low transmitter hardware complexity by requiring only one transmit RF chain. Also, spatial modulation receivers are fairly simple since multi-antenna interference is absent. Spatial modulation has been studied extensively in the literature. For a recent survey, see [5] and the references therein.

The low hardware complexity of spatial modulation comes at the cost of rate loss, since the available spatial degrees of freedom are under-utilized. Complete utilization of spatial degrees of freedom, as in conventional MIMO, requires using $n_t$ RF chains, leading to high hardware complexity. Generalized spatial modulation strikes a balance between spatial modulation and MIMO by using $K$ $(1 < K < n_t)$ RF chains and activating $K$ antennas per channel use [6], [7]. Indices of the $K$ active antennas as well as the symbols transmitted on them carry information. Several variants of spatial and generalized spatial modulation have been studied in the literature [8], [9]. The idea of index modulation has also been extended to other domains, such as indexing of sub-carriers and time-slots [10], [11], [2], [12]. Advanced OFDM index modulation schemes that improve performance over conventional sub-carrier index modulation are also studied in [13], [14], [15].

Knowledge of spectral efficiency is necessary for the design of modulation and coding. The work in [16] shows via simulations that spatial modulation with a single receive antenna can achieve higher capacity compared with SISO. The results of [16] are limited to single receive antenna systems, and the capacity computation involves evaluating a numerical integral for the rate conveyed by the index in addition to the expectation over fading. The work in [17] provides an approximation for the capacity of single receive antenna spatial modulation. The technique is highly specialized and there is no indication that it can be generalized either to spatial modulation with higher number of receive antennas or to generalized spatial modulation. The works in [18], [19], [20], [21], [22] derive approximations or bounds on capacity of spatial and generalized spatial modulation, but the results are not sufficiently tight for determining the parameters of modulation and coding. The works in [23], [24] state that the capacity of spatial modulation is equal to the number of receive antennas times the capacity of AWGN channel [23, Eq. (30)], [24, Eq. (15)], which on the face of it violates the MIMO bound on the degrees of freedom of the $2 \times n_r$ channels, for large $n_r$.

Calculating the spectral efficiency of index modulation is challenging in part because the vector-valued transmit signal is the product of two information-carrying variables, one choosing the index and the other representing the modulation symbol. A random channel coefficient matrix multiplies this product signal, which adds another layer of detail. The optimal distribution of the index and modulating signal is unknown; further, it is unknown if the optimal distribution is a product distribution (independent).

Our outer bounds for spatial modulation are a combination of the MIMO bound and a genie-aided SIMO bound. Our lower bound utilizes a chain rule decomposition, also used in [18], but with the important distinction that our calculation does not employ any further conditioning or approximation of the chain rule terms. The only departure of our lower bound from optimality is due to choosing a codebook distribution which has not been proved to be optimal. In contrast, [18] further approximates the antenna index term which can significantly weaken the inner bound, as demonstrated via numerical results. The work in [20] employs a Gaussian mixture model

This work was made possible in part by the grants 1718551 and 2008684 from the National Science Foundation.

The authors are with the Department of Electrical and Computer Engineering, The University of Texas at Dallas, Texas, United States, 75080. Email: {bharath.shamasundar, aria}@utdallas.edu

This article has been accepted for publication in a future issue of this journal, but has not been fully edited. Content may change prior to final publication. Citation information: DOI 10.1109/TWC.2022.3173207, IEEE Transactions on Wireless Communications



for the multi-antenna transmit signal and bounds its entropy. This approach performed well at high SNR, but lacks the facility to reliably bound the index modulation rate between MIMO and SIMO capacities, as one would hope and expect. In fact, numerical results show that it under-performs SIMO capacity at low-SNR. At high SNR, the lower bound of [20] has been the best in the literature, but nevertheless it is significantly improved by the present work. For example, for a $4 \times 2$ spatial modulation, at 8 bits/s/Hz, our bound is 2 dB tighter than [20]. Our contributions in this paper can be summarized as follows:

1) We derive bounds on the capacity of spatial modulation and show analytically that our lower and upper bounds meet at high-SNR when the number of receive antennas is greater than or equal to the number of transmit antennas, i.e., high-SNR capacity in these cases is completely characterized.
2) We extend our analysis to provide a comprehensive catalog of tight bounds for various index modulation schemes, namely, generalized spatial modulation (in frequency-flat and frequency-selective channels), time-index modulation, and frequency index modulation.
3) We provide performance upper limits for the practical class of techniques that encode the index and the modulation independently. When compared with our capacity lower bound, our upper bound for independent encoding circumscribes the suboptimality of uniform index codebooks and Gaussian modulation codebooks under the assumption of independent encoding.
4) Finally, we provide exhaustive simulation results illustrating our bounds under a variety of channel conditions. The results reveal that our bounds are significantly tighter than the previous bounds and approximations in the literature. Based on the simulations, we also make some important observations about when index modulation should be used in practice and when it should not be.

An early version of some results of this paper appeared in [25].

## II. Multi-Antenna Index Modulation

### A. $2 \times 1$ *Spatial Modulation*

Consider a $2 \times 1$ spatial modulation system shown in Fig. 1, in which information is conveyed through the index of the active antenna (captured by the variable $v$) and the symbol transmitted from the active antenna (denoted by $z$). The received signal is given by

$$y = g_1 z v + g_2 z(1-v) + w \tag{1}$$

$$= \begin{cases} g_1 z + w & \text{if } v = 1 \\ g_2 z + w & \text{if } v = 0 \end{cases} \tag{2}$$

where $w$ obeys $\mathcal{CN}(0, \sigma^2)$, and $g_1, g_2, w$ are independent of each other and of the inputs. An average transmit power constraint of $\sigma_z^2$ is assumed on $z$. We do not assume $z$ and $v$ are independent. $v$ is a Bernoulli random variable characterized with $\mathbb{P}(v = 1) = p$, and we define the signal-to-noise ratio parameter $\rho \triangleq \frac{\sigma_z^2}{\sigma^2}$. We denote by $h(\cdot)$ the entropy of

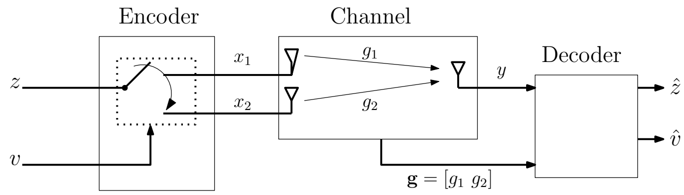


Fig. 1. Schematic diagram of $2 \times 1$ spatial modulation.

a (continuous or discrete) random variable. We denote by $C_{SISO}$ the capacity of SISO fading channel. We begin with the following elementary, but useful result.

**Proposition 1.** *The capacity of* $2 \times 1$ *spatial modulation satisfies the following bounds:*

$$C_{SISO} \leq C_{SM} \leq C_{SISO} + 1 \tag{3}$$

*Proof.* The lower-bound is a simple outcome of SISO being a special case of $2 \times 1$ spatial modulation (when spatial modulation elects to send no information via the index). Therefore, the capacity of spatial modulation is no less than SISO capacity.

To prove the upper bound, we have

$$I(v, z; y|g_1, g_2) = I(z; y|v, g_1, g_2) + I(v; y|g_1, g_2). \tag{4}$$

The first term is equivalent to the mutual information across a SISO channel with CSIR.

$$\begin{aligned} I(z; y|v, g_1, g_2) =& pI(z; y|v = 1, g_1, g_2) + \\ & (1-p) I(z; y|v = 0, g_1, g_2) \\ =& p\, I(x_1; y|g_1) + (1-p)\, I(x_2; y|g_2) \\ =& I(x_1; y|g_1) \qquad \text{(by symmetry)} \end{aligned} \tag{5}$$

Now consider the second term in (4)

$$\begin{aligned} I(v; y|g_1, g_2) &= h(v|g_1, g_2) - h(v|y, g_1, g_2) \\ &= h(v) - h(v|y, g_1, g_2), \end{aligned} \tag{6}$$

where the last equality is due to the independence of channel gains from input values. Combining Eqs. (4), (5), and (6)

$$I(v, z; y|g_1, g_2) = I(x_1; y|g_1) + h(v) - h(v|y, g_1, g_2) \tag{7}$$

It then follows that

$$\begin{aligned} C_{SM} &= \max_{p(v,z)} I(v, z; y|g_1, g_2) \\ &= \max_{p(v,z)} \left[ I(x_1; y|g_1) + h(v) - h(v|y, g_1, g_2) \right] \\ &\leq \max_{p(v,z)} \left[ I(x_1; y|g_1) + h(v) \right] \\ &\leq \max_{p(v,z)} I(x_1; y|g_1) + \max_{p(v,z)} h(v) \\ &= C_{SISO} + 1 \end{aligned}$$

□

*Remark* 1. It can be shown that the SISO lower bound is tight at low SNR, i.e., $\frac{C_{SM}}{C_{SISO}} \underset{\rho \to 0}{\longrightarrow} 1$, using a simple sandwich argument: MISO capacity upper bounds the spatial modulation capacity, and MISO capacity tends to SISO capacity at

This article has been accepted for publication in a future issue of this journal, but has not been fully edited. Content may change prior to final publication. Citation information: DOI 10.1109/TWC.2022.3173207, IEEE Transactions on Wireless Communications


low SNR (assuming CSIR but no CSIT) [26].[1] Also, since $C_{SISO} = \Theta(\log \rho)$, the ratio of lower and upper bounds goes to one in high-SNR limit.

We now offer a Lemma that provides insight into the behavior of index modulation decoding at high SNR.

**Lemma 1.**

$$h(v|z, y, g_1, g_2) \overset{\rho\to\infty}{\longrightarrow} 0 \tag{8}$$

*Proof.* Let $\epsilon, \epsilon' > 0$ be arbitrary positive constants. Consider $g_1$ and $g_2$ such that $|g_1 - g_2| > \epsilon$. Then, there exists $0 < \delta < 1$ such that

$$\mathbb{P}(|g_1 - g_2| > \epsilon) = 1 - \delta. \tag{9}$$

Now, consider $z = \sqrt{\rho} \cdot z'$, where $z' \sim \mathcal{CN}(0, 1)$. We consider a receiver strategy where we throw away the symbols with $|z'| < \epsilon'$. There exists $0 < \delta' < 1$ such that

$$\mathbb{P}(|z'| \geq \epsilon') = 1 - \delta'. \tag{10}$$

The $2 \times 1$ spatial modulation system model can be written as

$$y = (g_1 - g_2)vz + g_2 z + w.$$

It can be seen that, conditioned on $y$, $z$, $g_1$, and $g_2$, the effective SNR for the detection of $v$ is bounded below by:

$$\begin{cases} \epsilon^2 \epsilon'^2 \rho & \text{w.p. } (1-\delta)(1-\delta') \\ 0 & \text{w.p. } \delta + \delta' - \delta\delta' \triangleq \delta'' \end{cases}$$

We now argue in reverse by assigning arbitrary small values for $\delta, \delta'$ and hence for $\delta''$. This induces fixed values for $\epsilon, \epsilon'$ through Equations (9), (10). For these fixed values, we can increase $\rho$ sufficiently to make $\epsilon^2 \epsilon'^2 \rho$ as large as desired. Under these conditions, via symbol-by-symbol detection, the symbols with a positive SNR lower-bound will be correctly detected (because their SNR is made arbitrarily high as $\rho \to \infty$), therefore the overall probability of error is limited to the symbols that did not have a positive SNR guarantee, i.e.

$$\mathbb{P}(\hat{v} \neq v) \leq \delta'' \tag{11}$$

and as mentioned earlier, we can make $\delta''$ as small as desired. By data processing inequality:

$$h(v|y, z, g_1, g_2) \leq h(v|\hat{v}(y, z, g_1, g_2)), \tag{12}$$

where $\hat{v}(y, z, g_1, g_2)$ is the estimate of $v$. By Fano's inequality

$$\begin{aligned} h(v|\hat{v}(y, z, g_1, g_2)) &\leq H(\mathbb{P}(\hat{v} \neq v)) + \mathbb{P}(\hat{v} \neq v) \log_2(|\chi| - 1) \\ &= H(\mathbb{P}(\hat{v} \neq v)), \end{aligned} \tag{13}$$

where the equality follows since $|\chi| = 2$. Due to the continuity of $H(\cdot)$, Eq. (11) implies $H(\mathbb{P}(\hat{v} \neq v)) < \delta'''$ for a positive $\delta'''$ that can be made arbitrarily small. This, together with (12) and (13) completes the proof. □

*Remark* 2. Lemma 1 implies that in spatial modulation, at high-SNR, decoding of $z$ implies the decoding of the index $v$. This says that in the high-SNR regime, arbitrarily long sequences of antenna indices can be recovered at the receiver with negligible error, as long as the rate of the codebook $z$ is sufficiently small. This exposes the tension between the recovery of antenna indices on the one hand, and the rate for the codebook $z$ on the other hand, in the high-SNR regime.

[1]The tightness of the SISO lower bound can also be shown from first principles, but the sandwich argument is more compact and is presented here for brevity.

### B. $n_t \times n_r$ Spatial Modulation

Consider a multi-antenna system with $n_t$ transmit and $n_r$ receive antennas. The $n_t \times n_r$ spatial modulation activates a single transmit antenna in a channel use and transmits a symbol from the activated antenna. The system model for $n_t \times n_r$ spatial modulation can be written as

$$\mathbf{y} = \left( \sum_{i=1}^{n_t} \mathbf{g}_i v_i \right) z + \mathbf{w}, \tag{14}$$

where $\mathbf{g}_i$ is the channel gain vector from transmit antenna $i$ to $n_r$ receive antennas, $v_i$ is the antenna activation variable for antenna $i$ such that only one of the $v_i$ is one and the remaining are zero, and $\mathbf{w}$ is the $n_r \times 1$ noise vector with its entries being i.i.d $\mathcal{CN}(0, \sigma^2)$. The system model in (14) can be written as

$$\mathbf{y} = \mathbf{G}\mathbf{v}z + \mathbf{w}, \tag{15}$$

where $\mathbf{G} = [\mathbf{g}_1 \ \mathbf{g}_2 \ \cdots \ \mathbf{g}_{n_t}]$ and $\mathbf{v} = [v_1 \ v_2 \ \cdots \ v_{n_t}]^T$ such that $\mathbf{v} \in \{\mathbf{e}_i, \ i = 1, \ldots, n_t\}$ with $\mathbf{e}_i$ standard $n_t \times 1$ basis vectors. We define $p_i \triangleq \mathbb{P}(\mathbf{v} = \mathbf{e}_i)$ as the probability of activating antenna $i$. Let $\mathbf{x} = \mathbf{v}z = [x_1 x_2 \ldots x_{n_t}]^T$ denote the $n_t \times 1$ transmit vector. We denote by $C_{SIMO}$ the capacity of SIMO fading channel. With this, we have the following proposition on the capacity of $n_t \times n_r$ spatial modulation.

**Proposition 2.** *The capacity of $n_t \times n_r$ spatial modulation satisfies the following bounds:*

$$C_{SIMO} \leq C_{SM} \leq C_{SIMO} + \log_2 n_t. \tag{16}$$

*Proof.* The lower bound follows from the fact that SIMO is a special case of spatial modulation when it emits no information through the index. Therefore, the capacity of $n_t \times n_r$ spatial modulation is no less than the capacity of SIMO fading channel with same number of receive antennas.

For the upper bound, we have

$$I(\mathbf{v}, z; \mathbf{y}|\mathbf{G}) = I(z; \mathbf{y}|\mathbf{v}, \mathbf{G}) + I(\mathbf{v}; \mathbf{y}|\mathbf{G}). \tag{17}$$

The first term is equivalent to the mutual information of a SIMO channel with CSIR.

$$\begin{aligned} I(z; \mathbf{y}|\mathbf{v}, \mathbf{G}) &= \sum_{i=1}^{n_t} p_i I(z; \mathbf{y}|\mathbf{v} = \mathbf{e}_i, \mathbf{G}) \\ &= \sum_{i=1}^{n_t} p_i I(x_i; \mathbf{y}|\mathbf{G}) \\ &= I(x_1; \mathbf{y}|\mathbf{G}) \quad \text{(by symmetry)} \end{aligned} \tag{18}$$

Now consider the second term in (17)

$$\begin{aligned} I(\mathbf{v}; \mathbf{y}|\mathbf{G}) &= h(\mathbf{v}|\mathbf{G}) - h(\mathbf{v}|\mathbf{y}, \mathbf{G}). \\ &= h(\mathbf{v}) - h(\mathbf{v}|\mathbf{y}, \mathbf{G}), \end{aligned} \tag{19}$$

where the last equality follows from the independence of channel and inputs. Combining Eqs. (17), (18), (19)

$$I(\mathbf{v}, z; \mathbf{y}|\mathbf{G}) = I(x_1; \mathbf{y}|\mathbf{G}) + h(\mathbf{v}) - h(\mathbf{v}|\mathbf{y}, \mathbf{G}) \tag{20}$$

This article has been accepted for publication in a future issue of this journal, but has not been fully edited. Content may change prior to final publication. Citation information: DOI 10.1109/TWC.2022.3173207, IEEE Transactions on Wireless Communications



It then follows that

$$\begin{aligned} C_{SM} &= \max_{p(\mathbf{v},z)} I(\mathbf{v},z;\mathbf{y}|\mathbf{G}) \\ &= \max_{p(\mathbf{v},z)} \left[I(x_1;\mathbf{y}|\mathbf{G}) + h(\mathbf{v}) - h(\mathbf{v}|\mathbf{y},\mathbf{G})\right] \\ &\le \max_{p(\mathbf{v},z)} \left[I(x_1;\mathbf{y}|\mathbf{G}) + h(\mathbf{v})\right] \\ &\le \max_{p(\mathbf{v},z)} I(x_1;\mathbf{y}|\mathbf{G}) + \max_{p(\mathbf{v},z)} h(\mathbf{v}) \\ &= C_{SIMO} + \log_2 n_t. \end{aligned}$$

□

We refer to the above upper bound as the *genie-aided upper bound* since the bound can be achieved when the genie provides error-free version of index at the receiver.

*Remark* 3. Using similar arguments as in the previous section, it can be shown that the lower bound in Proposition 2 is tight at low-SNR. Also, the ratio of lower and upper bounds goes to one at high-SNR.

We now present a tighter lower bound on the capacity of spatial modulation.

**Proposition 3.** *(Spatial modulation - Capacity lower bound) The capacity of $n_t \times n_r$ spatial modulation is lower bounded as follows:*

$$\begin{aligned} C_{SM} \ge\; & C_{SIMO} + \log_2 n_t - \\ & \mathbb{E}_{\mathbf{y},\mathbf{G}}\left[\sum_{i=1}^{n_t} \frac{\log_2 \sum_{j=1}^{n_t} \sqrt{\frac{|\Sigma_i|}{|\Sigma_j|}} \exp\left(\frac{1}{2}\mathbf{y}^H(\Sigma_i^{-1} - \Sigma_j^{-1})\mathbf{y}\right)}{\sum_{j=1}^{n_t} \sqrt{\frac{|\Sigma_i|}{|\Sigma_j|}} \exp\left(\frac{1}{2}\mathbf{y}^H(\Sigma_i^{-1} - \Sigma_j^{-1})\mathbf{y}\right)}\right], \end{aligned} \tag{21}$$

*where* $\Sigma_i = \mathbf{g}_i\mathbf{g}_i^H\sigma_z^2 + \sigma^2\mathbf{I}_{n_r}$.

*Proof.* We have

$$I(\mathbf{v},z;\mathbf{y}|\mathbf{G}) = I(z;\mathbf{y}|\mathbf{v},\mathbf{G}) + I(\mathbf{v};\mathbf{y}|\mathbf{G})$$

Therefore,

$$C_{SM} = \max_{p(\mathbf{v},z)} I(\mathbf{v},z;\mathbf{y}|\mathbf{G}) \ge I(z;\mathbf{y}|\mathbf{v},\mathbf{G}) + I(\mathbf{v};\mathbf{y}|\mathbf{G}).$$

To evaluate the right-hand side,[2] consider the signalling where $\mathbf{v}$ and $z$ are independent, $z \sim \mathcal{CN}(0,\sigma_z^2)$, and $\mathbf{v}$ is selected uniformly. As seen before, when $z \sim \mathcal{CN}(0,\sigma_z^2)$, the mutual information $I(z;\mathbf{y}|\mathbf{v},\mathbf{G}) = C_{SIMO}$ and the above inequality becomes

$$\begin{aligned} C_{SM} &\ge C_{SIMO} + I(\mathbf{v};\mathbf{y}|\mathbf{G}) \\ &= C_{SIMO} + h(\mathbf{v}|\mathbf{G}) - h(\mathbf{v}|\mathbf{y},\mathbf{G}) \\ &= C_{SIMO} + \log_2 n_t - h(\mathbf{v}|\mathbf{y},\mathbf{G}). \end{aligned} \tag{22}$$

Now, we have

$$h(\mathbf{v}|\mathbf{y},\mathbf{G}) = \mathbb{E}_{\mathbf{y},\mathbf{G}}\left[-\sum_{i=1}^{n_t} p(\mathbf{v}=\mathbf{e}_i|\mathbf{y},\mathbf{G})\log_2 p(\mathbf{v}=\mathbf{e}_i|\mathbf{y},\mathbf{G})\right], \tag{23}$$

where

$$p(\mathbf{v}=\mathbf{e}_i|\mathbf{y},\mathbf{G}) = \frac{p(\mathbf{y}|\mathbf{v}=\mathbf{e}_i,\mathbf{G})p(\mathbf{v}=\mathbf{e}_i|\mathbf{G})}{\sum_{j=1}^{n_t} p(\mathbf{y}|\mathbf{v}=\mathbf{e}_j,\mathbf{G})p(\mathbf{v}=\mathbf{e}_j|\mathbf{G})}.$$

From the system model of $n_t \times n_r$ spatial modulation, we have

$$\mathbb{E}(\mathbf{y}|\mathbf{v}=\mathbf{e}_i,\mathbf{G}) = \mathbf{g}_i\mathbb{E}(z) + \mathbb{E}(w) = 0$$

and

$$\begin{aligned} \mathrm{Cov}(\mathbf{y}|\mathbf{v}=\mathbf{e}_i,\mathbf{G}) &= \mathbf{g}_i\mathbf{g}_i^H\mathbb{E}(|z|^2) + \sigma^2\mathbf{I}_{n_r} \\ &= \mathbf{g}_i\mathbf{g}_i^H\sigma_z^2 + \sigma^2\mathbf{I}_{n_r} \triangleq \Sigma_i. \end{aligned}$$

Therefore,

$$p(\mathbf{y}|\mathbf{v}=\mathbf{e}_i,\mathbf{G}) = \frac{1}{\sqrt{(2\pi)^{n_r}|\Sigma_i|}} \exp\left(-\frac{1}{2}\mathbf{y}^H\Sigma_i^{-1}\mathbf{y}\right),$$

and hence

$$\begin{aligned} p(\mathbf{v}=\mathbf{e}_i|\mathbf{y},\mathbf{G}) &= \frac{\frac{1}{\sqrt{|\Sigma_i|}}\exp\left(-\frac{1}{2}\mathbf{y}^H\Sigma_i^{-1}\mathbf{y}\right)}{\sum_{j=1}^{n_t}\frac{1}{\sqrt{|\Sigma_j|}}\exp\left(-\frac{1}{2}\mathbf{y}^H\Sigma_j^{-1}\mathbf{y}\right)} \\ &= \frac{1}{\sum_{j=1}^{n_t}\sqrt{\frac{|\Sigma_i|}{|\Sigma_j|}}\exp\left(\frac{1}{2}\mathbf{y}^H(\Sigma_i^{-1}-\Sigma_j^{-1})\mathbf{y}\right)}. \end{aligned}$$

Using this expression in (23) and substituting the resulting expression in (22) proves the proposition. □

We now show that for $n_r \ge n_t$, our capacity lower bound and genie-aided upper bound meet at high SNR, and therefore a full description of capacity has been achieved.

**Lemma 2.** *At high-SNR, $h(\mathbf{v}|\mathbf{y},\mathbf{G}) \to 0$ with probability one, when $n_r \ge n_t$.*

*Proof.* We have

$$h(\mathbf{v}|\mathbf{y},\mathbf{G}) = h(\mathbf{v}|\mathbf{G}\mathbf{v}z + \mathbf{w},\mathbf{G}).$$

Let $n_r \ge n_t$. Then, $\mathbf{G}$ has full column rank with probability one since its entries are drawn independently from a continuous distribution [27]. Also, for $\mathbf{G}$ with full column rank $\mathbf{G}^\dagger\mathbf{G} = \mathbf{I}_{n_t}$, where $\mathbf{G}^\dagger$ denotes the pseudoinverse of $\mathbf{G}$. Therefore, by data processing inequality

$$\begin{aligned} h(\mathbf{v}|\mathbf{G}\mathbf{v}z + \mathbf{w},\mathbf{G}) &\le h(\mathbf{v}|\mathbf{G}^\dagger\mathbf{G}\mathbf{v}z + \mathbf{G}^\dagger\mathbf{w}) \\ &= h(\mathbf{v}|\mathbf{v}z + \mathbf{G}^\dagger\mathbf{w}) \text{ with prob. 1} \end{aligned}$$

Now, $\mathbf{v}z + \mathbf{G}^\dagger\mathbf{w} \overset{\sigma^2\to 0}{\longrightarrow} \mathbf{v}z$ with probability one. Therefore,

$$h(\mathbf{v}|\mathbf{v}z + \mathbf{G}^\dagger\mathbf{w}) \overset{\sigma^2\to 0}{\longrightarrow} h(\mathbf{v}|\mathbf{v}z).$$

But $h(\mathbf{v}|\mathbf{v}z) = 0$ since $\mathbf{v}$ is fully specified by the position of non-zero and hence knowledge of $\mathbf{v}z$ fully reveals $\mathbf{v}$. This proves the lemma. □

Lemma 2 combined with (22) shows that our capacity lower bound meets the genie-aided upper bound at high-SNR for $n_r \ge n_t$. Lemma 2 also shows that the independent encoding of index and symbol is optimal at high SNR for $n_r \ge n_t$.

[2] So that any maximization of individual terms on the right hand side does not compromise the inequality, all mutual information terms on the right are calculated according to one and the same distribution.

This article has been accepted for publication in a future issue of this journal, but has not been fully edited. Content may change prior to final publication. Citation information: DOI 10.1109/TWC.2022.3173207, IEEE Transactions on Wireless Communications



*Remark* 4. (Spatial modulation - Upper bound for independent encoding)
Independent encoding of $\mathbf{v}$ and $z$ is an important and practically useful special case. For this case, the spectral efficiency satisfies the following bound:

$$I(\mathbf{v}, z; \mathbf{y}|\mathbf{G}) \leq C_{SIMO} + \log_2 n_t - \mathbb{E}_{\mathbf{y},z,\mathbf{G}}\left[\sum_{i=1}^{n_t} \frac{\log_2 \sum_{j=1}^{n_t} \exp\left(\frac{\|\mathbf{y}-\mathbf{g}_i z\|^2 - \|\mathbf{y}-\mathbf{g}_j z\|^2}{2\sigma^2}\right)}{\sum_{j=1}^{n_t} \exp\left(\frac{\|\mathbf{y}-\mathbf{g}_i z\|^2 - \|\mathbf{y}-\mathbf{g}_j z\|^2}{2\sigma^2}\right)}\right] \tag{24}$$

This can be shown as follows:

$$\begin{aligned} I(\mathbf{v}, z; \mathbf{y}|\mathbf{G}) &= I(z; \mathbf{y}|\mathbf{v}, \mathbf{G}) + I(\mathbf{v}; \mathbf{y}|\mathbf{G}) \\ &= I(z; \mathbf{y}|\mathbf{v}, \mathbf{G}) + h(\mathbf{v}|\mathbf{G}) - h(\mathbf{v}|\mathbf{y}, \mathbf{G}) \\ &\leq C_{SIMO} + \log_2 n_t - h(\mathbf{v}|\mathbf{y}, z, \mathbf{G}). \end{aligned} \tag{25}$$

Now,

$$h(\mathbf{v}|\mathbf{y}, z, \mathbf{G}) = \mathbb{E}_{\mathbf{y},z,\mathbf{G}}\Big[-\sum_{i=1}^{n_t} p(\mathbf{v} = \mathbf{e}_i|\mathbf{y}, z, \mathbf{G}) \times \log_2 p(\mathbf{v} = \mathbf{e}_i|\mathbf{y}, z, \mathbf{G})\Big], \tag{26}$$

where

$$\begin{aligned} p(\mathbf{v} = \mathbf{e}_i|\mathbf{y}, z, \mathbf{G}) &= \frac{p(\mathbf{y}|\mathbf{v} = \mathbf{e}_i, z, \mathbf{G}) p(\mathbf{v} = \mathbf{e}_i|z, \mathbf{G})}{p(\mathbf{y}|z, \mathbf{G})} \\ &= \frac{p(\mathbf{y}|\mathbf{v} = \mathbf{e}_i, z, \mathbf{G}) p(\mathbf{v} = \mathbf{e}_i|z, \mathbf{G})}{\sum_{j=1}^{n_t} p(\mathbf{y}|\mathbf{v} = \mathbf{e}_j, z, \mathbf{G}) p(\mathbf{v} = \mathbf{e}_j|z, \mathbf{G})} \end{aligned} \tag{27}$$

From the system model of $n_t \times n_r$ spatial modulation in (15), we have

$$\mathbb{E}(\mathbf{y}|\mathbf{v} = \mathbf{e}_i, z, \mathbf{G}) = \mathbf{g}_i z$$

and

$$\text{Cov}(\mathbf{y}|\mathbf{v} = \mathbf{e}_i, z, \mathbf{G}) = \sigma^2 \mathbf{I}_{n_r}.$$

Therefore,

$$p(\mathbf{y}|\mathbf{v} = \mathbf{e}_i, z, \mathbf{G}) = \frac{1}{\sqrt{(2\pi\sigma^2)^{n_r}}} \exp\left(-\frac{\|\mathbf{y} - \mathbf{g}_i z\|^2}{2\sigma^2}\right). \tag{28}$$

Assuming uniform distribution on index independent of transmitted signal

$$p(\mathbf{v} = \mathbf{e}_i|z, \mathbf{G}) = p(\mathbf{v} = \mathbf{e}_i) = \frac{1}{n_t}.$$

Using the above equations in (27), we get

$$\begin{aligned} p(\mathbf{v} = \mathbf{e}_i|\mathbf{y}, z, \mathbf{G}) &= \frac{\exp\left(-\frac{\|\mathbf{y}-\mathbf{g}_i z\|^2}{2\sigma^2}\right)}{\sum_{j=1}^{n_t} \exp\left(-\frac{\|\mathbf{y}-\mathbf{g}_j z\|^2}{2\sigma^2}\right)} \\ &= \frac{1}{\sum_{j=1}^{n_t} \exp\left(\frac{\|\mathbf{y}-\mathbf{g}_i z\|^2 - \|\mathbf{y}-\mathbf{g}_j z\|^2}{2\sigma^2}\right)}. \end{aligned}$$

Using this equation in (26) and substituting the resulting expression in (25) proves the result.

### *C. Generalized Spatial Modulation*

Consider an $n_t \times n_r$ multi-antenna system. Generalized spatial modulation uses $K$ $(1 \leq K \leq n_t)$ transmit RF chains and activates $K$ transmit antennas out of the $n_t$ available transmit antennas in a channel use. From the activated antennas, $K$ symbols $z_1, \ldots, z_K$ are transmitted. The system model for generalized spatial modulation can be written as

$$\mathbf{y} = \mathbf{G}\mathbf{V}\mathbf{z} + \mathbf{w}, \tag{29}$$

where $\mathbf{G} = [\mathbf{g_1}\ \mathbf{g_2}\ \cdots\ \mathbf{g}_{n_t}]$ is the $n_r \times n_t$ channel matrix with $\mathbf{g}_i$ being the channel gain vector from transmit antenna $i$ to $n_r$ receive antennas and $\mathbf{z} = [z_1, z_2, \ldots, z_K]^T$ is the $K \times 1$ vector of symbols transmitted from $K$ active antennas. As before, we assume an average transmit power constraint of $\sigma_z^2$. The matrix $\mathbf{V}$ is the $n_t \times K$ antenna activation matrix which, when multiplied by $\mathbf{G}$, extracts the $K$ columns of $\mathbf{G}$ corresponding to the $K$ active antennas. If transmit antenna $i$ corresponds to the activated antenna $j \in \{1, \ldots, K\}$, then $\mathbf{V}_{ij} = 1$, otherwise $\mathbf{V}_{ij} = 0$. There are $\binom{n_t}{K}$ distinct activation patterns, which we denote by $\{\mathbf{V}_1, \mathbf{V}_2, \ldots, \mathbf{V}_{\binom{n_t}{K}}\}$. We denote by $q_i \triangleq \mathbb{P}(\mathbf{V} = \mathbf{V}_i)$ the probability of each distinct activation pattern. We denote by $C_{MIMO}$ the capacity of $n_t \times n_r$ MIMO fading channel and by $C_{MIMO}^{K \times n_r}$ the capacity of $K \times n_r$ MIMO fading channel. Then, we have the following proposition on the capacity of generalized spatial modulation.

**Proposition 4.** *The capacity of $n_t \times n_r$ generalized spatial modulation with $K$ active antennas satisfies the following bounds:*

$$C_{MIMO}^{K \times n_r} \leq C_{GSM} \leq C_{MIMO}^{K \times n_r} + \log_2 \binom{n_t}{K}. \tag{30}$$

*Proof.* The lower bound follows from the fact that $K \times n_r$ MIMO is a special case of generalized spatial modulation when the transmitter chooses not to switch the active antennas. Therefore, the capacity of generalized spatial modulation is no less than the capacity of $K \times n_r$ MIMO fading channel.

For the upper bound, we have

$$I(\mathbf{V}, \mathbf{z}; \mathbf{y}|\mathbf{G}) = I(\mathbf{z}; \mathbf{y}|\mathbf{V}, \mathbf{G}) + I(\mathbf{V}; \mathbf{y}|\mathbf{G}). \tag{31}$$

The first term is equivalent to the mutual information of a $K \times n_r$ MIMO channel with CSIR.

$$\begin{aligned} I(\mathbf{z}; \mathbf{y}|\mathbf{V}, \mathbf{G}) &= \sum_{i=1}^{\binom{n_t}{K}} q_i I(\mathbf{z}; \mathbf{y}|\mathbf{V} = \mathbf{V}_i, \mathbf{G}) \\ &= I(\mathbf{z}; \mathbf{y}|\mathbf{V} = \mathbf{V}_1, \mathbf{G}) \quad \text{(by symmetry)} \end{aligned} \tag{32}$$

Now consider the second term in (31)

$$\begin{aligned} I(\mathbf{V}; \mathbf{y}|\mathbf{G}) &= h(\mathbf{V}|\mathbf{G}) - h(\mathbf{V}|\mathbf{y}, \mathbf{G}). \\ &= h(\mathbf{V}) - h(\mathbf{V}|\mathbf{y}, \mathbf{G}), \end{aligned} \tag{33}$$

where the last equality follows from the independence of channel and inputs. Combining Eqs. (31), (32), (33)

$$I(\mathbf{V}, \mathbf{z}; \mathbf{y}|\mathbf{G}) = I(\mathbf{z}; \mathbf{y}|\mathbf{V} = \mathbf{V}_1, \mathbf{G}) + h(\mathbf{V}) - h(\mathbf{V}|\mathbf{y}, \mathbf{G}) \tag{34}$$

This article has been accepted for publication in a future issue of this journal, but has not been fully edited. Content may change prior to final publication. Citation information: DOI 10.1109/TWC.2022.3173207, IEEE Transactions on Wireless Communications


It then follows that

$$\begin{aligned} C_{GSM} &= \max_{p(\mathbf{V},\mathbf{z})} I(\mathbf{V},\mathbf{z};\mathbf{y}|\mathbf{G}) \\ &= \max_{p(\mathbf{V},\mathbf{z})} \left[ I(\mathbf{z};\mathbf{y}|\mathbf{V}=\mathbf{V}_1,\mathbf{G}) + h(\mathbf{V}) - h(\mathbf{v}|\mathbf{y},\mathbf{G}) \right] \\ &\le \max_{p(\mathbf{V},\mathbf{z})} \left[ I(\mathbf{z};\mathbf{y}|\mathbf{V}=\mathbf{V}_1,\mathbf{G}) + h(\mathbf{V}) \right] \\ &\le \max_{p(\mathbf{V},\mathbf{z})} I(\mathbf{z};\mathbf{y}|\mathbf{V}=\mathbf{V}_1,\mathbf{G}) + \max_{p(\mathbf{V},\mathbf{z})} h(\mathbf{V}) \\ &= C_{MIMO}^{K\times n_r} + \log_2 \binom{n_t}{K}. \end{aligned}$$

□

We now present a tighter lower bound on the capacity of generalized spatial modulation.

**Proposition 5.** *(Generalized spatial modulation - Capacity lower bound)*
*The capacity of $n_t \times n_r$ generalized spatial modulation with $K$ active antennas is lower bounded as follows:*

$$C_{GSM} \ge C_{MIMO}^{K\times n_r} + \log_2 \binom{n_t}{K} - \mathbb{E}_{\mathbf{y},\mathbf{G}} \left[ \sum_{i=1}^{\binom{n_t}{K}} \frac{\log_2 \sum_{j=1}^{\binom{n_t}{K}} \sqrt{\frac{|\Gamma_i|}{|\Gamma_j|}} \exp\left( \frac{1}{2}\mathbf{y}^H(\Gamma_i^{-1} - \Gamma_j^{-1})\mathbf{y} \right)}{\sum_{j=1}^{\binom{n_t}{K}} \sqrt{\frac{|\Gamma_i|}{|\Gamma_j|}} \exp\left( \frac{1}{2}\mathbf{y}^H(\Gamma_i^{-1} - \Gamma_j^{-1})\mathbf{y} \right)} \right], \tag{35}$$

*where $\Gamma_i = \mathbf{G}\mathbf{V}_i\mathbf{V}_i^H\mathbf{G}^H\frac{\sigma_z^2}{K} + \sigma^2\mathbf{I}_{n_r}$.*

*Proof.* The proof is similar to the proof of Proposition 3. The main idea is that, for the evaluation of $I(\mathbf{z};\mathbf{y}|\mathbf{V},\mathbf{G}) + I(\mathbf{V};\mathbf{y}|\mathbf{G})$, we consider the signalling where $\mathbf{V}$ and $\mathbf{z}$ are independent, $\mathbf{z} \sim \mathcal{CN}(\mathbf{0}, \frac{\sigma_z^2}{K}\mathbf{I}_{n_r})$, and $\mathbf{V}$ is selected uniformly from $\{\mathbf{V}_i\}_{i=1}^{\binom{n_t}{K}}$. □

*Remark* 5. (Generalized spatial modulation - Upper bound for independent encoding)
It can be shown that the following bound holds on the spectral efficiency of generalized spatial modulation under independent encoding of $\mathbf{V}$ and $\mathbf{z}$:

$$I(\mathbf{V},\mathbf{z};\mathbf{y}|\mathbf{G}) \le C_{MIMO}^{K\times n_r} + \log_2 \binom{n_t}{K} - \mathbb{E}_{\mathbf{y},\mathbf{z},\mathbf{G}} \left[ \sum_{i=1}^{\binom{n_t}{K}} \frac{\log_2 \sum_{j=1}^{\binom{n_t}{K}} \exp\left( \frac{\|\mathbf{y}-\mathbf{G}\mathbf{V}_i\mathbf{z}\|^2 - \|\mathbf{y}-\mathbf{G}\mathbf{V}_j\mathbf{z}\|^2}{2\sigma^2} \right)}{\sum_{j=1}^{\binom{n_t}{K}} \exp\left( \frac{\|\mathbf{y}-\mathbf{G}\mathbf{V}_i\mathbf{z}\|^2 - \|\mathbf{y}-\mathbf{G}\mathbf{V}_j\mathbf{z}\|^2}{2\sigma^2} \right)} \right]. \tag{36}$$

## III. Multi-Antenna Index Modulation in Frequency Selective Channels

In this section, we extend the capacity results to frequency selective channels using MIMO-OFDM framework. Let $N$ denote the number of sub-carriers. The system model for $n_t \times n_r$ MIMO-OFDM in the frequency domain, after the removal of cyclic prefix, is given by [28]

$$\begin{bmatrix} \mathbf{y}(0) \\ \mathbf{y}(1) \\ \vdots \\ \mathbf{y}(N-1) \end{bmatrix} = \begin{bmatrix} \mathbf{G}(0) & & & \\ & \mathbf{G}(1) & & \\ & & \ddots & \\ & & & \mathbf{G}(N-1) \end{bmatrix} \begin{bmatrix} \mathbf{x}(0) \\ \mathbf{x}(1) \\ \vdots \\ \mathbf{x}(N-1) \end{bmatrix} + \begin{bmatrix} \mathbf{w}(0) \\ \mathbf{w}(1) \\ \vdots \\ \mathbf{w}(N-1) \end{bmatrix}, \tag{37}$$

where $\mathbf{y}(k)$ is the $n_r \times 1$ received signal on the sub-carrier $k$, $\mathbf{x}(k)$ is the $n_t \times 1$ transmit vector on the sub-carrier $k$, $\mathbf{G}(k)$ is the $n_r \times n_t$ flat fading channel response matrix corresponding to the sub-carrier $k$, and $\mathbf{w}(k) \sim \mathcal{CN}(\mathbf{0}, \sigma^2\mathbf{I}_{n_r})$ is the $n_r \times 1$ noise vector across the receive antennas on the sub-carrier $k$. The capacity of MIMO-OFDM when CSI is available at the receiver but not at the transmitter is given by [28]

$$\begin{aligned} C_{MIMO-OFDM} &= \max_{\{p(\mathbf{x}(k))\}_{k=0}^{N-1}} \frac{1}{N} \sum_{k=0}^{N-1} I(\mathbf{x}(k);\mathbf{y}(k)|\mathbf{G}(k)) \\ &= \mathbb{E}\left( \frac{1}{N} \sum_{k=0}^{N-1} \log_2 \left[ \det(\mathbf{I}_{n_r} + \rho\mathbf{G}(k)\mathbf{G}(k)^H) \right] \right), \end{aligned} \tag{38}$$

where $\rho = \frac{P}{\sigma^2 N n_t}$, with $P$ being the average transmit power per MIMO-OFDM symbol.

### A. OFDM-based Spatial Modulation

In OFDM-based spatial modulation, one of the $n_t$ transmit antennas is activated and an OFDM symbol is transmitted from the active antenna. Therefore,

$$\mathbf{x}(k) = \mathbf{v}z(k), \quad k = 0, \dots, N-1$$

where $z(k)$ is the symbol transmitted from the active antenna on the sub-carrier $k$ and $\mathbf{v} \in \{\mathbf{e}_i\}_{i=1}^{n_t}$ such that the selected $\mathbf{v}$ is the same for all $k = 0, \dots, N-1$. Therefore, the system model for OFDM-based spatial modulation can be written as in Eq. (39). This can be compactly written as

$$\mathbf{y} = \mathbf{G}\mathbf{W}\mathbf{z} + \mathbf{w}, \tag{40}$$

where $\mathbf{W} \in \{\mathbf{W}_i\}_{i=1}^{n_t}$ with $\mathbf{W}_i = \text{diag}\{\mathbf{e}_i, \mathbf{e}_i, \dots, \mathbf{e}_i\}$ and $\mathbf{z} = [z(0), z(1), \dots, z(N-1)]^T$. The capacity of OFDM-based spatial modulation is then given by

$$C_{SM} = \max_{p(\mathbf{W},\mathbf{z})} \frac{1}{N} I(\mathbf{W},\mathbf{z};\mathbf{y}|\mathbf{G}).$$

Note that, the mutual information is normalized by $N$ since $N$ symbols are transmitted in one OFDM frame. With this, we have the following results on the capacity of OFDM-based spatial modulation.

**Proposition 6.** *The capacity of OFDM-based spatial modulation satisfies the following bounds:*

$$C_{SIMO-OFDM} \le C_{SM} \le C_{SIMO-OFDM} + \frac{1}{N}\log_2 n_t \tag{41}$$

*Proof.* The proof is similar to Proposition 2 and is omitted for brevity. □

**Proposition 7.** *(OFDM-based spatial modulation - Capacity lower bound)*
*The capacity of $n_t \times n_r$ OFDM-based spatial modulation satisfies the lower bound in Eq.* (42)*, where $\Sigma_i(k) = \frac{\sigma_z^2}{N}\mathbf{g}_i(k)\mathbf{g}_i(k)^H + \sigma^2\mathbf{I}_{n_r}$.*

*Proof.* The proof is similar to Proposition 3 and is omitted for brevity. □

*Remark* 6. (OFDM-based spatial modulation - Upper bound for independent encoding)
The bound in Eq. (43) on the next page holds for independent encoding of $\mathbf{W}$ and $\mathbf{z}$.

### B. OFDM-based Generalized Spatial Modulation

To carryout generalized spatial modulation in frequency selective channels, $K$ out of the $n_t$ transmit antennas are activated and $K$ OFDM symbols are transmitted from the active antennas. Therefore,

$$\mathbf{x}(k) = \mathbf{V}\mathbf{z}(k), \quad k = 0, \ldots, N-1$$

where $\mathbf{z}(k) = [z_1(k), z_2(k), \ldots, z_K(k)]^T$ is the symbol vector transmitted from the $K$ active antennas on the sub-carrier $k$ and $\mathbf{V} \in \{\mathbf{V}_i\}_{i=1}^{\binom{n_t}{K}}$ ($\mathbf{V}_i$ is the antenna activation matrix as discussed in previous section) such that the selected $\mathbf{V}$ is the same for all $k = 0, \ldots, N-1$. Therefore, the system model for OFDM-based generalized spatial modulation can be written as in Eq. (44) (next page). This can be compactly written as

$$\mathbf{y} = \mathbf{G}\mathbf{U}\mathbf{z} + \mathbf{w}, \tag{45}$$

where $\mathbf{U} \in \{\mathbf{U}_i\}_{i=1}^{\binom{n_t}{K}}$ with $\mathbf{U}_i = \text{diag}\{\mathbf{V}_i, \mathbf{V}_i, \ldots, \mathbf{V}_i\}$ and $\mathbf{z} = [\mathbf{z}(0), \mathbf{z}(1), \ldots, \mathbf{z}(N-1)]^T$. With this system model, the capacity of OFDM-based generalized spatial modulation is

$$C_{GSM} = \max_{p(\mathbf{U},\mathbf{z})} \frac{1}{N} I(\mathbf{U}, \mathbf{z}; \mathbf{y}|\mathbf{G}).$$

We have the following propositions on the spectral efficiency of OFDM-based generalized spatial modulation.

**Proposition 8.** *The capacity of $n_t \times n_r$ OFDM-based generalized spatial modulation with $K$ active antennas satisfies the following bounds:*

$$C_{MIMO-OFDM}^{K\times n_r} \leq C_{GSM} \leq C_{MIMO-OFDM}^{K\times n_r} + \frac{1}{N}\log_2\binom{n_t}{K} \tag{46}$$

**Proposition 9.** *(OFDM-based generalized spatial modulation - Capacity lower bound)*
*The capacity of $n_t \times n_r$ OFDM-based generalized spatial modulation with $K$ active antennas satisfies the lower bound in Eq.* (47) *on page 9, where $\Gamma_i(k) = \frac{\sigma_z^2}{KN}\mathbf{G}(k)\mathbf{V}_i\mathbf{V}_i^H\mathbf{G}(k)^H + \sigma^2\mathbf{I}_{n_r}$.*

The proofs are similar to developments in Section II-C and are omitted for brevity.

*Remark* 7. (OFDM-based generalized spatial modulation - Upper bound for independent encoding) It can be shown that the spectral efficiency of OFDM-based generalized spatial modulation with independent encoding of $\mathbf{U}$ and $\mathbf{z}$ satisfies the bound in Eq. (48) on page 9.

## IV. Spectral Efficiency of Time and Frequency Index Modulation

In addition to multi-antenna index modulation, several time and frequency index modulation techniques are proposed in the literature (see [10], [11], [2], [12], [29] and references therein). We consider the basic versions of time and frequency index modulations and present the spectral efficiency bounds on them. The aim of this section is to illustrate that time and frequency index modulations share same mathematical structure as multi-antenna index modulations and therefore the analysis in the previous sections extend to time and frequency index modulations as well.

### A. Frequency Index Modulation

Frequency index modulation is built on OFDM in which a subset of sub-carriers is selected from the total available sub-carriers and modulation symbols are transmitted on the selected (active) sub-carriers. The choice of the active sub-carriers also carries a part of information in addition to the

$$\begin{bmatrix} \mathbf{y}(0) \\ \mathbf{y}(1) \\ \vdots \\ \mathbf{y}(N-1) \end{bmatrix} = \begin{bmatrix} \mathbf{G}(0) & & & \\ & \mathbf{G}(1) & & \\ & & \ddots & \\ & & & \mathbf{G}(N-1) \end{bmatrix} \begin{bmatrix} \mathbf{v} & & & \\ & \mathbf{v} & & \\ & & \ddots & \\ & & & \mathbf{v} \end{bmatrix} \begin{bmatrix} z(0) \\ z(1) \\ \vdots \\ z(N-1) \end{bmatrix} + \begin{bmatrix} \mathbf{w}(0) \\ \mathbf{w}(1) \\ \vdots \\ \mathbf{w}(N-1) \end{bmatrix} \tag{39}$$

$$C_{SM} \geq C_{SIMO-OFDM} + \frac{1}{N}\log_2 n_t - \frac{1}{N}\mathbb{E}_{\mathbf{y},\mathbf{G}}\left[\sum_{i=1}^{n_t} \frac{\log_2 \sum_{j=1}^{n_t}\prod_{k=0}^{N-1}\sqrt{\frac{|\Sigma_i(k)|}{|\Sigma_j(k)|}}\exp\left(\frac{1}{2}\mathbf{y}(k)^H(\Sigma_i^{-1}(k) - \Sigma_j^{-1}(k))\mathbf{y}(k)\right)}{\sum_{j=1}^{n_t}\prod_{k=0}^{N-1}\sqrt{\frac{|\Sigma_i(k)|}{|\Sigma_j(k)|}}\exp\left(\frac{1}{2}\mathbf{y}(k)^H(\Sigma_i^{-1}(k) - \Sigma_j^{-1}(k))\mathbf{y}(k)\right)}\right] \tag{42}$$

information carried by the transmitted symbols. Specifically, out of the $N$ available sub-carriers in the OFDM, $N_a$ sub-carriers are activated and $N_a$ symbols are emitted on the active sub-carriers. This is sometimes also referred to as sub-carrier index modulation. The spectral efficiency of frequency index modulation with $M$-ary symbol constellation is studied in [30]. In this section, we study the spectral efficiency of frequency index modulation without restricting to finite symbol constellation.

We now provide the system model of frequency index modulation and present the spectral efficiency bounds. The frequency domain OFDM system model in matrix form is given by

$$\begin{bmatrix} y(0) \\ y(1) \\ \vdots \\ y(N-1) \end{bmatrix} = \begin{bmatrix} G(0) & & & \\ & G(1) & & \\ & & \ddots & \\ & & & G(N-1) \end{bmatrix} \begin{bmatrix} x(0) \\ x(1) \\ \vdots \\ x(N-1) \end{bmatrix} + \begin{bmatrix} w(0) \\ w(1) \\ \vdots \\ w(N-1) \end{bmatrix}, \tag{49}$$

where $x(k)$ and $y(k)$ are the transmitted and received signals on sub-carrier $k$, respectively, $G(k)$ is the channel response corresponding to sub-carrier $k$, and $w(k) \sim \mathcal{CN}(0, \sigma^2)$ is the noise on sub-carrier $k$. This can be written compactly as

$$\mathbf{y} = \mathbf{G}\mathbf{x} + \mathbf{w}.$$

Note that the system model above has the same form as the multi-antenna model except that the channel matrix is diagonal. The frequency index modulation activates $N_a$ out of the $N$ sub-carriers, and therefore the transmit vector has the form

$$\mathbf{x} = \mathbf{V}\mathbf{z},$$

where $\mathbf{z} = [z(1), z(2), \ldots, z(N_a)]^T$ is the vector of transmitted symbols on $N_a$ active sub-carriers and $\mathbf{V}$ is the sub-carrier activation matrix which is constructed in exactly the same way as the antenna activation matrix in generalized spatial modulation, with the role of antennas taken by the sub-carriers in the frequency index modulation. The system model for frequency index modulation can therefore be written as

$$\mathbf{y} = \mathbf{G}\mathbf{V}\mathbf{z} + \mathbf{w}.$$

There are $\binom{N}{N_a}$ possible sub-carrier activation matrices denoted by $\{\mathbf{V}_i\}_{i=1}^{\binom{N}{N_a}}$. Since the transmission of OFDM symbol is carried out in $N$ channel uses, the capacity of frequency index modulation is given by

$$C_{FIM} = \max_{p(\mathbf{V},\mathbf{z})} \frac{1}{N} I(\mathbf{V}, \mathbf{z}; \mathbf{y}|\mathbf{G}).$$

It can be seen that the system model of frequency index modulation is similar to that of generalized spatial modulation, and therefore, using the similar arguments as before, bounds on spectral efficiency can be derived for frequency index modulation. Hence, for brevity we now present without proofs the bounds on spectral efficiency of frequency index modulation. In the following propositions, $C_{OFDM}^{N_a}$ denotes the capacity of the OFDM system which activates first $N_a$ sub-carriers out of the $N$ sub-carriers, leaving the remaining $N - N_a$ sub-carriers unused. That is,

$$C_{OFDM}^{N_a} = \mathbb{E}\Big[\frac{1}{N} \sum_{k=0}^{N_a-1} \log_2\big(1 + \frac{\sigma_z^2}{\sigma^2 N_a} |G(k)|^2\big)\Big],$$

where $\sigma_z^2$ is the average transmit power per OFDM frame.

**Proposition 10.** *The capacity of frequency index modulation with $N_a$ active sub-carriers out of $N$ sub-carriers satisfies the following bounds:*

$$C_{OFDM}^{N_a} \leq C_{FIM} \leq C_{OFDM}^{N_a} + \frac{1}{N} \log_2 \binom{N}{N_a}. \tag{50}$$

**Proposition 11.** *(Frequency index modulation - Capacity lower bound)*
*The capacity of frequency index modulation with $N_a$ active*

---

$$\frac{1}{N} I(\mathbf{W}, \mathbf{z}; \mathbf{y}|\mathbf{G}) \leq C_{SIMO-OFDM} + \frac{1}{N}\log_2 n_t - \frac{1}{N}\mathbb{E}_{\mathbf{y},\mathbf{z},\mathbf{G}}\left[\sum_{i=1}^{n_t} \frac{\log_2 \sum_{j=1}^{n_t} \prod_{k=0}^{N-1} \exp\left(\frac{\|\mathbf{y}(k)-\mathbf{g}_i(k)z(k)\|^2 - \|\mathbf{y}(k)-\mathbf{g}_j(k)z(k)\|^2}{2\sigma^2}\right)}{\sum_{j=1}^{n_t} \prod_{k=0}^{N-1} \exp\left(\frac{\|\mathbf{y}(k)-\mathbf{g}_i(k)z(k)\|^2 - \|\mathbf{y}(k)-\mathbf{g}_j(k)z(k)\|^2}{2\sigma^2}\right)}\right] \tag{43}$$

$$\begin{bmatrix} \mathbf{y}(0) \\ \mathbf{y}(1) \\ \vdots \\ \mathbf{y}(N-1) \end{bmatrix} = \begin{bmatrix} \mathbf{G}(0) & & & \\ & \mathbf{G}(1) & & \\ & & \ddots & \\ & & & \mathbf{G}(N-1) \end{bmatrix} \begin{bmatrix} \mathbf{V} & & & \\ & \mathbf{V} & & \\ & & \ddots & \\ & & & \mathbf{V} \end{bmatrix} \begin{bmatrix} \mathbf{z}(0) \\ \mathbf{z}(1) \\ \vdots \\ \mathbf{z}(N-1) \end{bmatrix} + \begin{bmatrix} \mathbf{w}(0) \\ \mathbf{w}(1) \\ \vdots \\ \mathbf{w}(N-1) \end{bmatrix} \tag{44}$$

This article has been accepted for publication in a future issue of this journal, but has not been fully edited. Content may change prior to final publication. Citation information: DOI 10.1109/TWC.2022.3173207, IEEE Transactions on Wireless Communications


*sub-carriers out of $N$ sub-carriers is lower bounded as follows:*

$$C_{FIM} \geq C_{OFDM}^{N_a} + \frac{1}{N}\log_2\binom{N}{N_a} - \frac{1}{N}\mathbb{E}_{\mathbf{y},\mathbf{G}}\left[\sum_{i=1}^{\binom{N}{N_a}} \log_2 \frac{\sum_{j=1}^{\binom{N}{N_a}} \sqrt{\frac{|\Gamma_i|}{|\Gamma_j|}}\exp\left(\frac{1}{2}\mathbf{y}^H(\Gamma_i^{-1}-\Gamma_j^{-1})\mathbf{y}\right)}{\sum_{j=1}^{\binom{N}{N_a}} \sqrt{\frac{|\Gamma_i|}{|\Gamma_j|}}\exp\left(\frac{1}{2}\mathbf{y}^H(\Gamma_i^{-1}-\Gamma_j^{-1})\mathbf{y}\right)}\right], \tag{51}$$

*where* $\Gamma_i = \mathbf{G}\mathbf{V}_i\mathbf{V}_i^H\mathbf{G}^H\frac{\sigma_z^2}{N_a} + \sigma^2\mathbf{I}_N$.

*Remark* 8. (Frequency index modulation - Upper bound for independent encoding)
The spectral efficiency of frequency index modulation when $\mathbf{V}$ and $\mathbf{z}$ are independent satisfies the following bound:

$$\frac{1}{N}I(\mathbf{V},\mathbf{z}:\mathbf{y}|\mathbf{G}) \leq C_{OFDM}^{N_a} + \frac{1}{N}\log_2\binom{N}{N_a} - \frac{1}{N}\mathbb{E}_{\mathbf{y},\mathbf{z},\mathbf{G}}\left[\sum_{i=1}^{\binom{N}{N_a}} \log_2 \frac{\sum_{j=1}^{\binom{N}{N_a}} \exp\left(\frac{\|\mathbf{y}-\mathbf{G}\mathbf{V}_i z\|^2-\|\mathbf{y}-\mathbf{G}\mathbf{V}_j\mathbf{z}\|^2}{2\sigma^2}\right)}{\sum_{j=1}^{\binom{N}{N_a}} \exp\left(\frac{\|\mathbf{y}-\mathbf{G}\mathbf{V}_i z\|^2-\|\mathbf{y}-\mathbf{G}\mathbf{V}_j\mathbf{z}\|^2}{2\sigma^2}\right)}\right]. \tag{52}$$

### B. Time Index Modulation

In time index modulation, time is divided into frames of $T$ time-slots. Out of the $T$ time-slots, $T_a$ time-slots are activated and modulation symbols are transmitted in the active time-slots. The remaining $T - T_a$ time-slots are inactive and no data is transmitted. The choice of the active time-slots also carries information in addition to the information carried by the modulation symbols. We assume a quasi-static flat-fading channel that remains constant for any given frame and can change from frame to frame. The system model for time index modulation is then given by

$$\begin{bmatrix} y(0) \\ y(1) \\ \vdots \\ y(T-1) \end{bmatrix} = \begin{bmatrix} g & & & \\ & g & & \\ & & \ddots & \\ & & & g \end{bmatrix} \begin{bmatrix} x(0) \\ x(1) \\ \vdots \\ x(T-1) \end{bmatrix} + \begin{bmatrix} w(0) \\ w(1) \\ \vdots \\ w(T-1) \end{bmatrix}, \tag{53}$$

which can be compactly written as

$$\mathbf{y} = \mathbf{G}\mathbf{x} + \mathbf{w}.$$

Here, the input vector $\mathbf{x}$ has the form

$$\mathbf{x} = \mathbf{V}\mathbf{z},$$

where $\mathbf{V}$ is the $T \times T_a$ time-slot activation matrix and $\mathbf{z}$ is the $T_a \times 1$ vector containing the symbols transmitted in the $T_a$ active slots. The time-slot activation matrix $\mathbf{V}$ is constructed in exactly the same way as the antenna activation matrix in generalized spatial modulation with the role of antennas taken by the time-slots. Therefore, the system model of time index modulation can be written as

$$\mathbf{y} = \mathbf{G}\mathbf{V}\mathbf{z} + \mathbf{w}. \tag{54}$$

There are $\binom{T}{T_a}$ possible time-slot activation matrices denoted by $\{\mathbf{V}_i\}_{i=1}^{\binom{T}{T_a}}$. The capacity of time-index modulation is given by

$$C_{TIM} = \max_{p(\mathbf{V},\mathbf{z})} \frac{1}{T} I(\mathbf{V},\mathbf{z};\mathbf{y}|\mathbf{G}).$$

Since the system model for time index modulation is similar to that of generalized spatial modulation, the spectral efficiency bounds can be easily obtained using the analysis presented earlier. For brevity, we now present without proof the bounds on the spectral efficiency of time index modulation. In the following results, we denote by $C_{SISO}(\rho)$ the capacity of SISO fading channel with signal-to-noise ratio $\rho$. That is, $C_{SISO}(\rho) = \mathbb{E}_g(1+\rho|g|^2)$. Also, we denote by $\sigma_z^2$ the average transmit power per frame.

---

$$C_{GSM} \geq C_{MIMO-OFDM}^{K\times n_r} + \frac{1}{N}\log_2\binom{n_t}{K} - \frac{1}{N}\mathbb{E}_{\mathbf{y},\mathbf{G}}\left[\sum_{i=1}^{\binom{n_t}{K}} \log_2 \frac{\sum_{j=1}^{\binom{n_t}{K}}\prod_{k=0}^{N-1} \sqrt{\frac{|\Gamma_i(k)|}{|\Gamma_j(k)|}}\exp\left(\frac{1}{2}\mathbf{y}(k)^H(\Gamma_i^{-1}(k)-\Gamma_j^{-1}(k))\mathbf{y}(k)\right)}{\sum_{j=1}^{\binom{n_t}{K}}\prod_{k=0}^{N-1} \sqrt{\frac{|\Gamma_i(k)|}{|\Gamma_j(k)|}}\exp\left(\frac{1}{2}\mathbf{y}(k)^H(\Gamma_i^{-1}(k)-\Gamma_j^{-1}(k))\mathbf{y}(k)\right)}\right] \tag{47}$$

$$\frac{1}{N}I(\mathbf{U},\mathbf{z};\mathbf{y}|\mathbf{G}) \leq C_{MIMO-OFDM}^{K\times n_r} + \frac{1}{N}\log_2\binom{n_t}{K} - \frac{1}{N}\mathbb{E}_{\mathbf{y},\mathbf{z},\mathbf{G}}\left[\sum_{i=1}^{\binom{n_t}{K}} \log_2 \frac{\sum_{j=1}^{\binom{n_t}{K}}\prod_{k=0}^{N-1} \exp\left(\frac{\|\mathbf{y}(k)-\mathbf{G}(k)\mathbf{V}_i\mathbf{z}(k)\|^2-\|\mathbf{y}(k)-\mathbf{G}(k)\mathbf{V}_j\mathbf{z}(k)\|^2}{2\sigma^2}\right)}{\sum_{j=1}^{\binom{n_t}{K}}\prod_{k=0}^{N-1} \exp\left(\frac{\|\mathbf{y}(k)-\mathbf{G}(k)\mathbf{V}_i\mathbf{z}(k)\|^2-\|\mathbf{y}(k)-\mathbf{G}(k)\mathbf{V}_j\mathbf{z}(k)\|^2}{2\sigma^2}\right)}\right] \tag{48}$$

This article has been accepted for publication in IEEE Transactions on Wireless Communications. This is the author's version which has not been fully edited and content may change prior to final publication. Citation information: DOI 10.1109/TWC.2022.3173207
This article has been accepted for publication in a future issue of this journal, but has not been fully edited. Content may change prior to final publication. Citation information: DOI 10.1109/TWC.2022.3173207, IEEE Transactions on Wireless Communications


**Proposition 12.** *The capacity of time index modulation with $T_a$ active time-slots out of $T$ time-slots satisfies the following bounds:*

$$\frac{T_a}{T}C_{SISO}\left(\frac{\sigma_z^2}{\sigma^2 T_a}\right) \leq C_{TIM} \leq \frac{T_a}{T}C_{SISO}\left(\frac{\sigma_z^2}{\sigma^2 T_a}\right) + \frac{1}{T}\log_2\binom{T}{T_a}. \quad (55)$$

**Proposition 13.** *(Time index modulation - Capacity lower bound)*
*The capacity of time index modulation with $T_a$ active time-slots out of $T$ time-slots is lower bounded as follows:*

$$C_{TIM} \geq \frac{T_a}{T}C_{SISO}\left(\frac{\sigma_z^2}{\sigma^2 T_a}\right) + \frac{1}{T}\log_2\binom{T}{T_a} - \frac{1}{T}\mathbb{E}_{\mathbf{y},\mathbf{G}}\left[\sum_{i=1}^{\binom{T}{T_a}} \log_2 \frac{\sum_{j=1}^{\binom{T}{T_a}} \sqrt{\frac{|\Gamma_i|}{|\Gamma_j|}} \exp\left(\frac{1}{2}\mathbf{y}^H(\Gamma_i^{-1} - \Gamma_j^{-1})\mathbf{y}\right)}{\sum_{j=1}^{\binom{T}{T_a}} \sqrt{\frac{|\Gamma_i|}{|\Gamma_j|}} \exp\left(\frac{1}{2}\mathbf{y}^H(\Gamma_i^{-1} - \Gamma_j^{-1})\mathbf{y}\right)}\right], \quad (56)$$

*where* $\Gamma_i = \mathbf{G}\mathbf{V}_i\mathbf{V}_i^H\mathbf{G}^H\frac{\sigma_z^2}{T_a} + \sigma^2\mathbf{I}_T$.

*Remark* 9. (Time index modulation - Upper bound for independent encoding)
The spectral efficiency of time index modulation when $\mathbf{V}$ and $\mathbf{z}$ are independent satisfies the following bound:

$$\frac{1}{T}I(\mathbf{V},\mathbf{z}:\mathbf{y}|\mathbf{G}) \leq \frac{T_a}{T}C_{SISO}\left(\frac{\sigma_z^2}{\sigma^2 T_a}\right) + \frac{1}{T}\log_2\binom{T}{T_a} - \frac{1}{T}\mathbb{E}_{\mathbf{y},\mathbf{z},\mathbf{G}}\left[\sum_{i=1}^{\binom{T}{T_a}} \log_2 \frac{\sum_{j=1}^{\binom{T}{T_a}} \exp\left(\frac{\|\mathbf{y}-\mathbf{G}\mathbf{V}_i\mathbf{z}\|^2 - \|\mathbf{y}-\mathbf{G}\mathbf{V}_j\mathbf{z}\|^2}{2\sigma^2}\right)}{\sum_{j=1}^{\binom{T}{T_a}} \exp\left(\frac{\|\mathbf{y}-\mathbf{G}\mathbf{V}_i\mathbf{z}\|^2 - \|\mathbf{y}-\mathbf{G}\mathbf{V}_j\mathbf{z}\|^2}{2\sigma^2}\right)}\right]. \quad (57)$$

*Remark* 10. Time-index modulation can also be carried out in frequency-selective channels by using the cyclic-prefixed single-carrier transmission as done in [12]. The analysis for this case closely follows that of generalized spatial modulation, and is therefore omitted here for brevity.

## V. Simulation Results

This section provides extensive simulation results under various channel conditions demonstrating the tightness and usefulness of our bounds.

### *A. Multi-Antenna Index Modulation in Rayleigh, Rician, and Nakagami Flat-Fading Channels*

Figure 2 shows the bounds on the spectral efficiency of $4\times4$ spatial modulation in Rayleigh flat-fading channel. It can be seen that our capacity lower bound meets the genie-aided upper bound at high-SNR which illustrates the tightness of our bounds. This also suggests that independent encoding of index and symbol can be optimal at high-SNR. Also, the capacity lower bound and MIMO upper bound are tight at low-SNR. The figure also shows that our upper bound on independent encoding is close to the capacity lower bound, which says that the uniform index codebook and Gaussian symbol codebook assumed in the capacity lower bound is not too sub-optimal under independent encoding. Further, it can be seen that, while the spectral efficiency of $4\times4$ spatial modulation is slightly higher than the $1\times4$ SIMO capacity, it is significantly lesser than the $4\times4$ MIMO capacity at high-SNR. This observation suggests that spatial modulation should only be considered when there is a strict hardware limitation that allows using only one RF chain. Using spatial modulation when there is no such hardware constraint is spectrally inefficient.

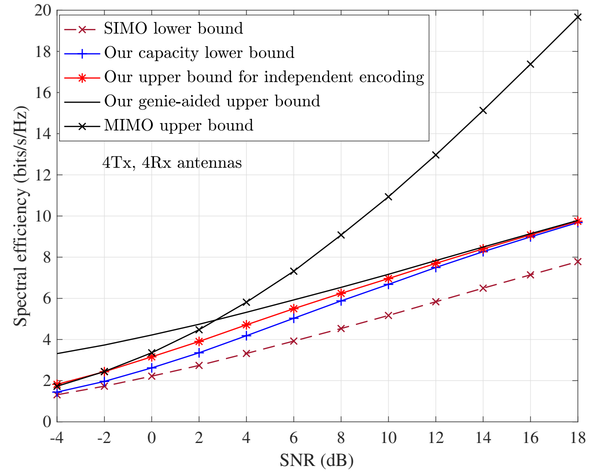


Fig. 2. Spectral efficiency bounds for $4\times4$ spatial modulation in Rayleigh fading channel.

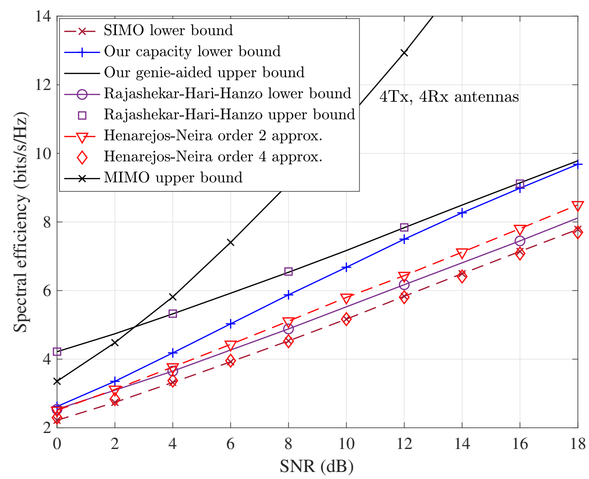


Fig. 3. Comparing bounds of the present paper with the bounds in [18] and approximations in [19] for $4\times4$ spatial modulation.

Figure 3 compares the capacity results of the present paper with those of [18] and [19]. The bounds in [18] are shown as Rajashekar-Hari-Hanzo lower and upper bounds. The capacity approximations in [19] using the Taylor series are shown as Henarejos-Neira order 2 and 4 approximations. It can be seen from Fig. 3 that, while the upper bound in [18] is identical

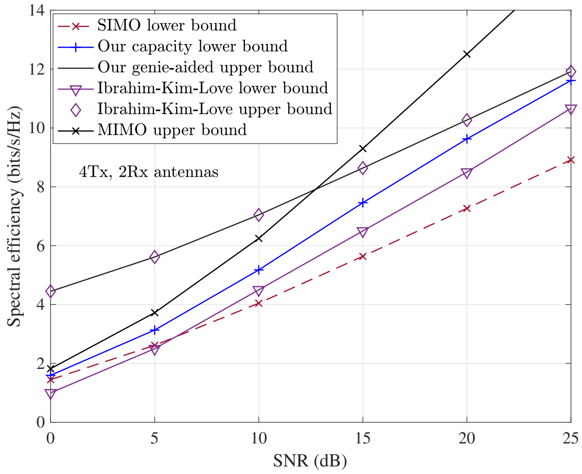


Fig. 4. Comparing bounds of the present paper with the bounds in [20] for $4 \times 2$ spatial modulation.

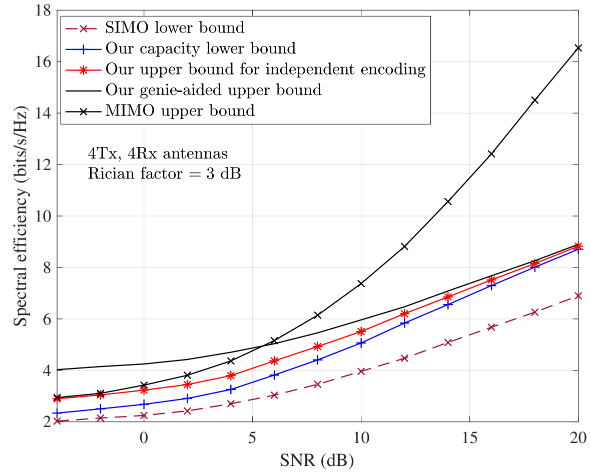


Fig. 6. Spectral efficiency bounds for $4 \times 4$ spatial modulation in Rician fading channel with Rician factor of 3 dB.

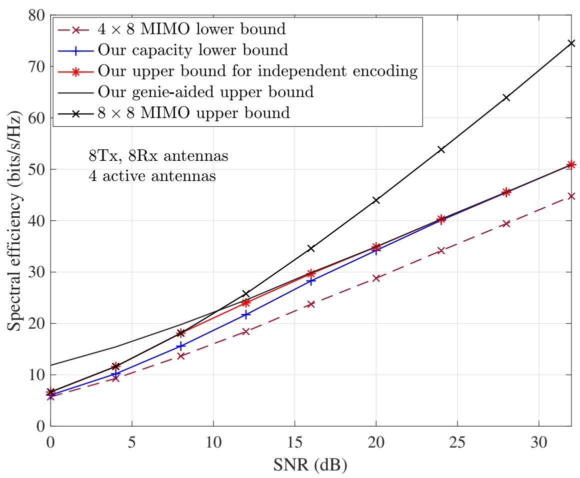


Fig. 5. Spectral efficiency bounds for $8 \times 8$ generalized spatial modulation in Rayleigh fading channel.

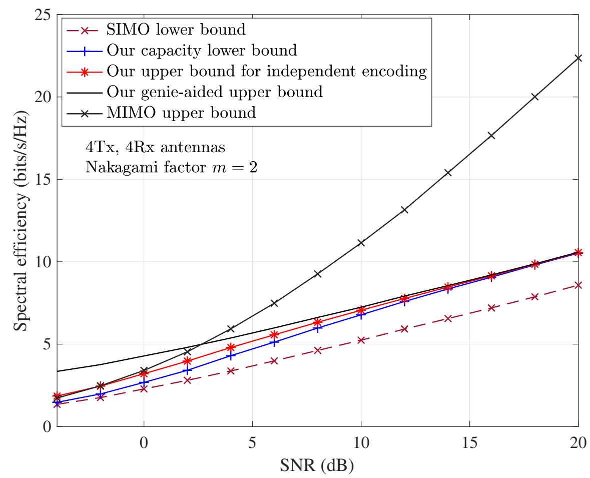


Fig. 7. Spectral efficiency bounds for $4 \times 4$ spatial modulation in Nakagami-$m$ fading channel with $m = 2$.

with our genie-aided upper bound, the lower bound is weaker compared to our independence lower bound at all SNR values. For example, at 8 bits/s/Hz, our lower bound is 5 dB tighter than the lower bound in [18]. It can also be observed that the approximations of [19] are weaker compared to the bounds of the present paper.

Figure 4 compares the capacity bounds of the present paper with the bounds in [20] for $4 \times 2$ spatial modulation. The bounds in [20] are shown as Ibrahim-Kim-Love upper and lower bounds. It can be seen that the upper bound of [20] is identical with our genie-aided upper bound. However, the lower bound of [20] is weaker than our independence lower bound. For example, at 8 bits/s/Hz, our lower bound is 2 dB tighter than the lower bound in [20].

Figure 5 shows the spectral efficiency bounds for $8 \times 8$ generalized spatial modulation with 4 active antennas in Rayleigh flat-fading channel. It can be seen that our lower and upper bounds are tight at high-SNR. It can also be observed that at high-SNR the generalized spatial modulation achieves about 6 bits/s/Hz gain compared to the $4 \times 8$ MIMO (which uses the same number of RF chains as generalized spatial modulation). However, the spectral efficiency of generalized spatial modulation falls significantly below the $8 \times 8$ MIMO capacity. This again suggests that generalized spatial modulation is spectrally efficient in situations where there is a constraint on the number of RF chains. When there is no such hardware constraint MIMO should be preferred to generalized spatial modulation.

Figures 6 and 7 show the spectral efficiency bounds for spatial modulation in the Rician and Nakagami fading channels, respectively. Similarly, Figs. 8 and 9 show the spectral efficiency bounds for generalized spatial modulation in Rician and Nakagami fading channels, respectively. Similar observations as in Rayleigh fading channel can be made from these figures.

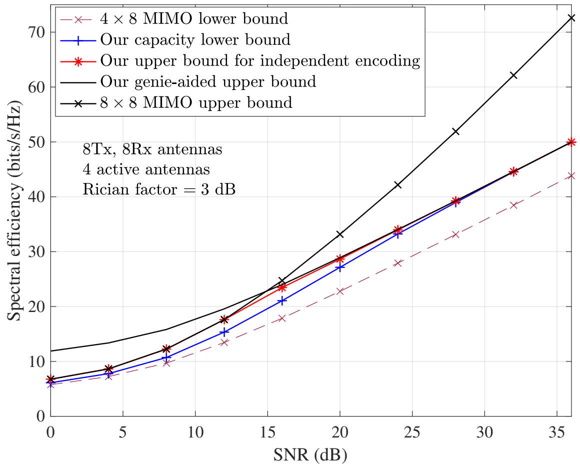


Fig. 8. Spectral efficiency bounds for $8 \times 8$ generalized spatial modulation in Rician fading channel with Rician factor of 3 dB.

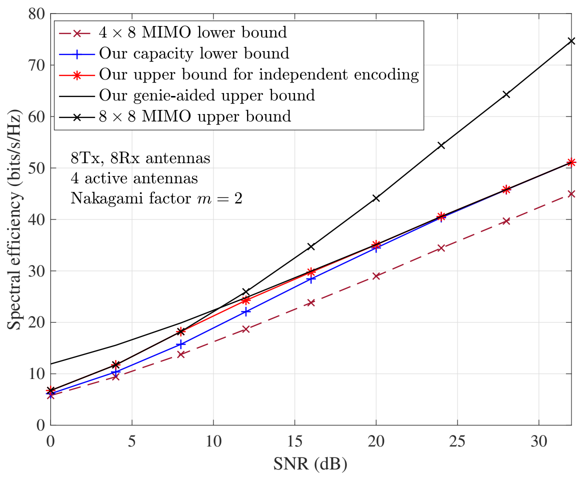


Fig. 9. Spectral efficiency bounds for $8 \times 8$ generalized spatial modulation in Nakagami-$m$ fading channel with $m = 2$.

## *B. Multi-Antenna Index Modulation in Frequency Selective Channels*

Figure 10 shows the spectral efficiency bounds for $4 \times 4$ OFDM-based spatial modulation using 16 sub-carriers. Our lower and upper bounds can be seen to be tight at all SNR. The figure also shows that the gain in spectral efficiency compared to SIMO-OFDM is small (fraction of a dB). This is because the antenna selection is done only once for the entire OFDM symbol (to retain low hardware complexity), which limits the amount of information conveyed by the index. Also, compared to MIMO-OFDM the spectral efficiency of OFDM-based spatial modulation is significantly lesser at high-SNR. Similar observations can be made from Fig. 11 which shows the spectral efficiency bounds for $8 \times 8$ OFDM-based generalized spatial modulation with four active antennas using 16 sub-carriers.

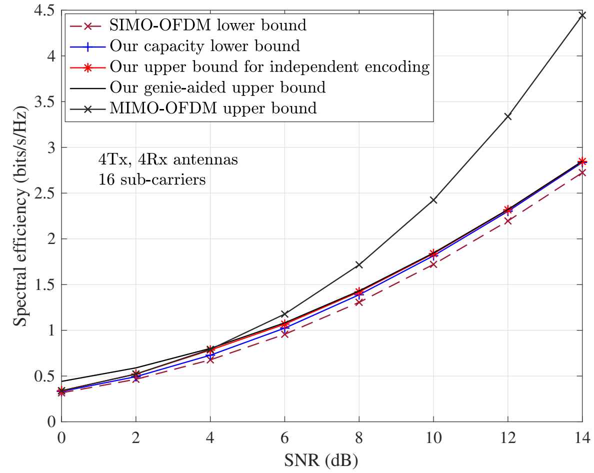


Fig. 10. Spectral efficiency bounds for $4 \times 4$ OFDM-based spatial modulation.

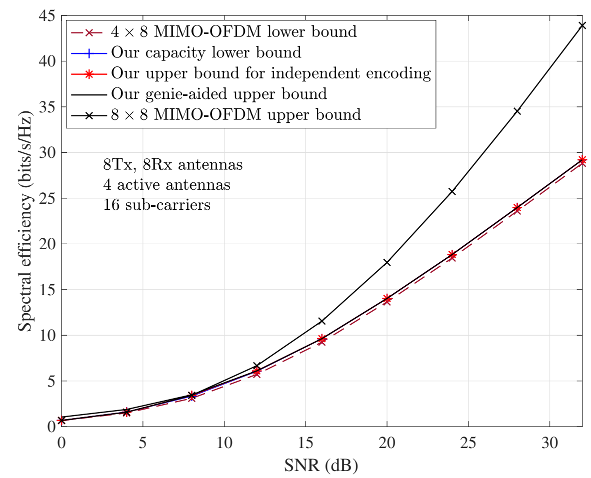


Fig. 11. Spectral efficiency bounds for $8 \times 8$ OFDM-based generalized spatial modulation.

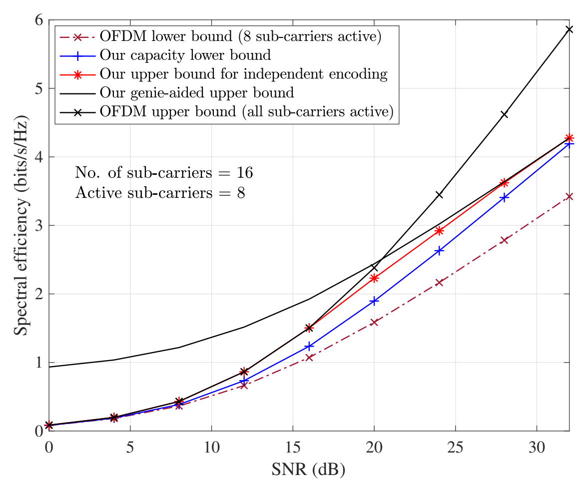


Fig. 12. Spectral efficiency bounds for frequency index modulation.

This article has been accepted for publication in a future issue of this journal, but has not been fully edited. Content may change prior to final publication. Citation information: DOI 10.1109/TWC.2022.3173207, IEEE Transactions on Wireless Communications



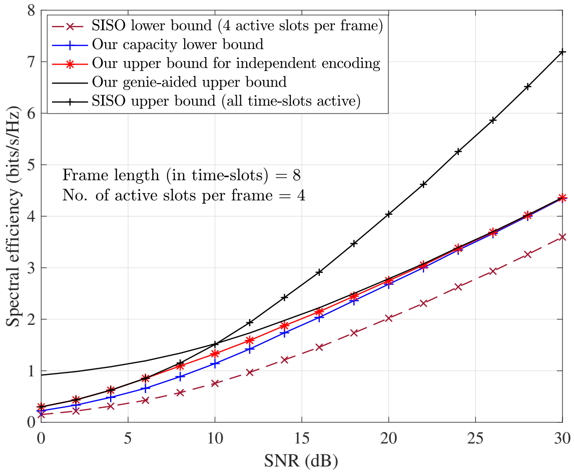


Fig. 13. Spectral efficiency bounds for time index modulation.

### C. Time and Frequency Index Modulation

Figure 12 shows spectral efficiency bounds for frequency index modulation using 16 sub-carriers out of which 8 sub-carriers are activated. There is a slight gain in spectral efficiency of frequency index modulation compared to an OFDM system which uses 8 sub-carriers leaving the remaining 8 sub-carriers unused (shown as OFDM lower bound in the figure). However, the spectral efficiency of the OFDM system where all the sub-carriers are used (shown as OFDM upper bound in the figure) is significantly higher than that of frequency index modulation at high-SNR. This suggests that the bandwidth should not be wasted either by leaving sub-channels vacant or by sub-carrier indexing as this leads to significant loss of spectral efficiency.

Figure 13 shows the bounds on spectral efficiency of time index modulation with a frame length of 8 time-slots of which 4 slots are used for transmitting the data. It can be seen that while there is a gain in spectral efficiency compared to a scheme that leaves 4 time-slots unused in each frame (shown as SISO lower bound in the figure), there is a significant loss in spectral efficiency compared to the conventional SISO transmission that uses all time-slots of the frame (shown as SISO upper bound in the figure). This suggests that time-indexing should be used only if there is a practical need for leaving certain time-slots vacant. Using time-indexing when there is no such need leads to a waste of time resource and is spectrally inefficient.

## VI. Discussion and Conclusion

This paper presented accurate bounds on the capacity of index modulation techniques. We presented a lower bound by evaluating the terms in a chain rule decomposition of mutual information under a uniformly distributed index and a Gaussian modulation variable that are independent of each other. We provided a genie-aided upper bound, where the genie provides an error-free version of the index to the receiver. When the number of receive antennas is bigger than or equal to the number of transmit antennas, our inner and outer bounds are proven to be tight at high SNR. We also provided an upper bound for capacity subject to the constraint of independent encoding of the index and the modulation variables. A catalog of results for spatial modulation, generalized spatial modulation, and time and frequency index modulation are provided.

Our results showed that independent encoding is optimal at low SNR and, for $n_r \geq n_t$, also optimal at high SNR. At other SNR, numerical results suggested that independent encoding is not far from optimal. However, the optimality (or lack thereof) of independent signaling/coding for the modulation variable and index variable remains an open problem.

## References

[1] E. Basar, "Index modulation techniques for 5G wireless networks," *IEEE Communications Magazine*, vol. 54, no. 7, pp. 168–175, 2016.

[2] E. Basar, M. Wen, R. Mesleh, M. Di Renzo, Y. Xiao, and H. Haas, "Index modulation techniques for next-generation wireless networks," *IEEE Access*, vol. 5, pp. 16 693–16 746, 2017.

[3] R. Y. Mesleh, H. Haas, S. Sinanovic, C. W. Ahn, and S. Yun, "Spatial modulation," *IEEE Transactions on Vehicular Technology*, vol. 57, no. 4, pp. 2228–2241, 2008.

[4] M. Di Renzo, H. Haas, A. Ghrayeb, S. Sugiura, and L. Hanzo, "Spatial modulation for generalized MIMO: Challenges, opportunities, and implementation," *Proceedings of the IEEE*, vol. 102, no. 1, pp. 56–103, 2014.

[5] M. Wen, B. Zheng, K. J. Kim, M. Di Renzo, T. A. Tsiftsis, K. Chen, and N. Al-Dhahir, "A survey on spatial modulation in emerging wireless systems: Research progresses and applications," *IEEE Journal on Selected Areas in Communications*, vol. 37, no. 9, pp. 1949–1972, 2019.

[6] T. Datta and A. Chockalingam, "On generalized spatial modulation," in *2013 IEEE Wireless Communications and Networking Conference (WCNC)*, 2013, pp. 2716–2721.

[7] T. L. Narasimhan, P. Raviteja, and A. Chockalingam, "Generalized spatial modulation in large-scale multiuser mimo systems," *IEEE Transactions on Wireless Communications*, vol. 14, no. 7, pp. 3764–3779, 2015.

[8] R. Mesleh, S. S. Ikki, and H. M. Aggoune, "Quadrature spatial modulation," *IEEE Transactions on Vehicular Technology*, vol. 64, no. 6, pp. 2738–2742, 2014.

[9] Y. Bian, X. Cheng, M. Wen, L. Yang, H. V. Poor, and B. Jiao, "Differential spatial modulation," *IEEE Transactions on Vehicular Technology*, vol. 64, no. 7, pp. 3262–3268, 2014.

[10] E. Başar, Ü. Aygölü, E. Panayırcı, and H. V. Poor, "Orthogonal frequency division multiplexing with index modulation," *IEEE Transactions on signal processing*, vol. 61, no. 22, pp. 5536–5549, 2013.

[11] R. Abu-alhiga and H. Haas, "Subcarrier-index modulation OFDM," in *2009 IEEE 20th International Symposium on Personal, Indoor and Mobile Radio Communications*, 2009, pp. 177–181.

[12] B. Shamasundar, S. Bhat, S. Jacob, and A. Chockalingam, "Multidimensional index modulation in wireless communications," *IEEE Access*, vol. 6, pp. 589–604, 2017.

[13] M. Wen, B. Ye, E. Basar, Q. Li, and F. Ji, "Enhanced orthogonal frequency division multiplexing with index modulation," *IEEE Transactions on Wireless Communications*, vol. 16, no. 7, pp. 4786–4801, 2017.

[14] T. Mao, Z. Wang, Q. Wang, S. Chen, and L. Hanzo, "Dual-mode index modulation aided ofdm," *IEEE Access*, vol. 5, pp. 50–60, 2016.

[15] M. Wen, E. Basar, Q. Li, B. Zheng, and M. Zhang, "Multiple-mode orthogonal frequency division multiplexing with index modulation," *IEEE Transactions on Communications*, vol. 65, no. 9, pp. 3892–3906, 2017.

[16] Y. Yang and B. Jiao, "Information-guided channel-hopping for high data rate wireless communication," *IEEE Communications Letters*, vol. 12, no. 4, pp. 225–227, 2008.

[17] E. Faregh, M. Eslami, and J. Haghighat, "A closed-form mutual information approximation for multiple-antenna systems with spatial modulation," *IEEE Wireless Communications Letters*, vol. 5, no. 6, pp. 636–639, 2016.

[18] R. Rajashekar, K. Hari, and L. Hanzo, "Reduced-complexity ML detection and capacity-optimized training for spatial modulation systems," *IEEE Transactions on Communications*, vol. 62, no. 1, pp. 112–125, 2014.

This article has been accepted for publication in a future issue of this journal, but has not been fully edited. Content may change prior to final publication. Citation information: DOI 10.1109/TWC.2022.3173207, IEEE Transactions on Wireless Communications



[19] P. Henarejos and A. I. Pérez-Neira, "Capacity analysis of index modulations over spatial, polarization, and frequency dimensions," *IEEE Transactions on Communications*, vol. 65, no. 12, pp. 5280–5292, 2017.

[20] A. A. I. Ibrahim, T. Kim, and D. J. Love, "On the achievable rate of generalized spatial modulation using multiplexing under a Gaussian mixture model," *IEEE Transactions on Communications*, vol. 64, no. 4, pp. 1588–1599, 2016.

[21] T. Lakshmi Narasimhan and A. Chockalingam, "On the capacity and performance of generalized spatial modulation," *IEEE Communications Letters*, vol. 20, no. 2, pp. 252–255, 2016.

[22] L. Xiao, P. Xiao, Z. Liu, W. Yu, H. Haas, and L. Hanzo, "A compressive sensing assisted massive sm-vblast system: Error probability and capacity analysis," *IEEE Transactions on Wireless Communications*, vol. 19, no. 3, pp. 1990–2005, 2020.

[23] A. Younis and R. Mesleh, "Information-theoretic treatment of space modulation MIMO systems," *IEEE Transactions on Vehicular Technology*, vol. 67, no. 8, pp. 6960–6969, 2018.

[24] A. Younis, N. Abuzgaia, R. Mesleh, and H. Haas, "Quadrature spatial modulation for 5G outdoor millimeter–wave communications: Capacity analysis," *IEEE Transactions on Wireless Communications*, vol. 16, no. 5, pp. 2882–2890, 2017.

[25] B. Shamasundar and A. Nosratinia, "Spectral efficiency of multi-antenna index modulation," in *2021 IEEE International Symposium on Information Theory (ISIT)*, 2021, pp. 3291–3295.

[26] D. Tse and P. Viswanath, *Fundamentals of wireless communication*. Cambridge university press, 2005.

[27] X. Feng and Z. Zhang, "The rank of a random matrix," *Applied Mathematics and Computation*, vol. 185, no. 1, pp. 689–694, 2007. [Online]. Available: https://www.sciencedirect.com/science/article/pii/S0096300306009040

[28] H. Bolcskei, D. Gesbert, and A. J. Paulraj, "On the capacity of ofdm-based spatial multiplexing systems," *IEEE Transactions on Communications*, vol. 50, no. 2, pp. 225–234, 2002.

[29] B. Shamasundar, S. Jacob, and A. Chockalingam, "Time-indexed media-based modulation," in *2017 IEEE 85th Vehicular Technology Conference (VTC Spring)*, 2017, pp. 1–5.

[30] M. Wen, X. Cheng, M. Ma, B. Jiao, and H. V. Poor, "On the achievable rate of ofdm with index modulation," *IEEE Transactions on Signal Processing*, vol. 64, no. 8, pp. 1919–1932, 2016.

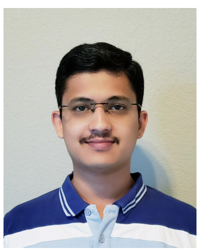

**Bharath Shamasundar** received the Bachelor of Engineering degree in Electronics and Communications from Siddaganga Institute of Technology, Tumkur, India in 2014. He received the M.Sc.(Engg.) and Ph.D. degrees in Electrical Communications Engineering from Indian Institute of Science, Bangalore, India in 2020. Presently, he is working as a postdoctoral research associate at the University of Texas at Dallas, United States. His research interests lie broadly in the areas of wireless communications, information theory, and machine learning.

**Aria Nosratinia** (S'87, M'97, SM'04, F'10) is Erik Jonsson Distinguished Professor and associate head of the electrical engineering department at the University of Texas at Dallas. He received his Ph.D. in Electrical and Computer Engineering from the University of Illinois at Urbana-Champaign in 1996. He has held visiting appointments at Princeton University, Rice University, and UCLA. His interests lie in the broad area of information theory and signal processing, with applications in wireless communications, data security and privacy. Dr. Nosratinia is a fellow of IEEE for contributions to multimedia and wireless communications. He has served as editor and area editor for the IEEE Transactions on Wireless Communications, and editor for the IEEE Transactions on Information Theory, IEEE Transactions on Image Processing, IEEE Signal Processing Letters, IEEE Wireless Communications (Magazine), and Journal of Circuits, Systems, and Computers. He has received the National Science Foundation career award, and the outstanding service award from the IEEE Signal Processing Society, Dallas Chapter. He has served as the secretary of the IEEE information theory society, treasurer for ISIT, publications chair for the IEEE Signal Processing Workshop, as well as member of the technical committee for a number of conferences. He was the general co-chair of IEEE Information Theory Workshop in 2018. Dr. Nosratinia is a registered professional engineer in the state of Texas and a Clarivate Analytics highly cited researcher.